Band offsets and transitivity of $In_{1-x}Ga_xAs/In_{1-y}Al_yAs/InP$ heterostructures

J. Böhrer, A. Krost, T. Wolf, and D. Bimberg
Technische Universität Berlin, Institut für Festkörperphysik I, Hardenbergstrasse 36, D-1000 Berlin 12, Federal Republic of Germany
(Received 12 June 1992)

$In_{1-x}Ga_xAs/In_{1-y}Al_yAs$ quantum wells (QW's) and $In_{1-y}Al_yAs$ layers slightly lattice mismatched to InP substrates are grown by metalorganic chemical-vapor deposition and studied by calorimetric absorption spectroscopy (CAS), photoluminescence (PL), double-crystal x-ray diffractometry (DXD), and Shubnikov–de Haas (SdH) measurements. The layer compositions and the strain are directly determined from DXD. The strain partly relaxes selection rules and forbidden transitions, which are more sensitive to the relative conduction-band discontinuities $\Delta E_c/\Delta E_g$ than the allowed ones, appear in the CAS spectra of the QW's. Comparing the energies of the transitions with detailed band-structure calculations the relative conduction-band discontinuity $\Delta E_c/\Delta E_g$ is determined to be $(72\pm4)\%$ for $In_{0.540}Ga_{0.460}As/In_{0.531}Al_{0.469}As$. PL spectra of the type-II heterostructure $In_{0.489}Al_{0.511}As/InP$ show apart from the band-gap emissions two spatially indirect transitions across the $In_{1-y}Al_yAs/InP$ interface at 1.240 eV ($n=1$) and at 1.271 eV ($n=2$). The conduction-band discontinuity is determined from the energies of these transitions and SdH experiments in conjunction with self-consistent band-structure calculations for lattice-matched $In_{0.52}Al_{0.48}As$ to be $\Delta E_c=252$ meV or $\Delta E_c=2.86\Delta E_g$. From these results, the three conduction-band discontinuities $In_{1-x}Ga_xAs/InP$, $InP/In_{1-y}Al_yAs$, and $In_{1-y}Al_yAs/In_{1-x}Ga_xAs$ are found to be transitive.

$In_{0.53}Ga_{0.47}As/In_{0.52}Al_{0.48}As$ heterostructures lattice matched to InP are particularly attractive for high-performance electronic and photonic devices[1,2] as well as for future optoelectronic integrated circuits, because of the large difference of band gaps ($\Delta E_g=700$ meV at 300 K). The conduction-band discontinuity is approximately twice as large as for $In_{0.53}Ga_{0.47}As/InP$ leading to improved electron localization, e.g., in quantum-well devices or two-dimensional (2D) field-effect transistors. Interpretation of optical and electrical experiments and modeling of such devices requires precise knowledge of the ratio of conduction-band ΔE_c and valence-band ΔE_v discontinuities, since carrier transport both along and across the interfaces is strongly dependent on its magnitude. Presently, there are large discrepancies between the published values of $\Delta E_c/\Delta E_g$ for the $In_{0.53}Ga_{0.47}As/In_{0.52}Al_{0.48}As$ heterostructure; they range from $\Delta E_c=420$ meV $\hat{=}\Delta E_c/\Delta E_g=60\%$ to $\Delta E_c=695$ meV $\hat{=}\Delta E_c/\Delta E_g=85\%$.[3–11] For the $In_{0.52}Al_{0.48}As/InP$ type-II heterostructure, the values for the conduction-band discontinuity ΔE_c vary between 380 and 448 meV.[12–15]

In this paper we report a precise determination of ΔE_c for both $In_{1-x}Ga_xAs/In_{1-y}Al_yAs$ and $In_{1-y}Al_yAs/InP$ heterostructures. Our results are based on a comparative study by double-crystal x-ray diffractometry (DXD), photoluminescence, and calorimetric absorption spectroscopy. Each transition energy is carefully compared to predictions of band-structure calculations. The band-structure calculations used for the $In_{1-x}Ga_xAs/In_{1-y}Al_yAs$ quantum wells (QW's) are based on a finite square-well model including effects due to strain caused by lattice mismatch and due to the nonparabolicity of the conduction band, and recent exciton binding-energy calculations.[16] The band structure of the $In_{1-y}Al_yAs/InP$ heterostructures is calculated in a self-consistent way, solving the coupled Schrödinger and Poisson equations.

The experiments are performed on samples grown by low-pressure metalorganic chemical vapor deposition. They consist of a $In_{1-x}Ga_xAs/In_{1-y}Al_yAs$ multi-quantum-well (MQW) structure with $L_z=5$ nm, $L_b=20$ nm repreated ten times. A 50-nm $In_{1-y}Al_yAs$ buffer layer is grown first on the (100) semi-insulating Fe-doped InP substrate. The $In_{1-y}Al_yAs/InP$ heterostructures consisted of a 250-nm InP buffer and a 1-μm-thick $In_{1-y}Al_yAs$ layer. Trimethylmetals (TMGa, TMAl, and TMIn) and 100% arsine (AsH_3) and phosphine (PH_3) are used as starting materials. The growth temperature is 640 °C and the growth rate is about 0.35 nm/s.

Precise knowledge of the strain induced by a slight lattice mismatch and of the chemical composition of the layers is mandatory for a correct interpretation of the optical spectra. We have investigated the structural properties using DXD. In our DXD setup, an InP crystal is used as a first crystal. Experiments are carried out nondispersively in the $(+n,-n)$ mode with the Cu $K\alpha_1$ line. The results are compared to simulated DXD rocking curves using a kinematical step model as outlined by Segmüller and Blakeslee.[17] In Fig. 1 the experimental (dotted line) and the simulated (solid line) (400) x-ray rocking curves of a $In_{1-x}Ga_xAs/In_{1-y}Al_yAs$ MQW structure are depicted. Because of the background noise of the DXD setup, a background level of 80 counts are added to the simulation. Using the symmetric (400) reflection, we can monitor most sensitively the deviation

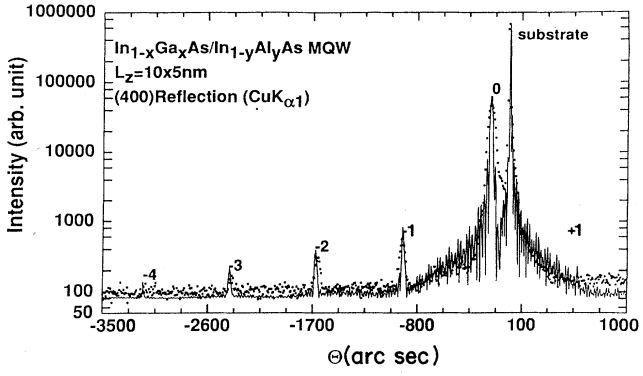

FIG. 1. X-ray rocking curve of $In_{1-x}Ga_xAs/In_{1-y}Al_yAs$ measured using DXD. Experimental results are shown as dots and the theoretical line-shape fit derived from kinematical theory as a solid line.

of the lattice constant $\Delta a_\perp$ perpendicular to the (100) interface plane. The average lattice mismatch of the QW structure as a whole to the InP substrate is obtained from the angle separation between the substrate and the main epilayer peak (zeroth-order peak). The average lattice mismatch to the InP substrate in this sample is $\Delta a_\perp/a = 1.24\times10^{-3}$. In addition, higher-order satellite peaks on one side are observed, which reflect the periodicity of the sample structure. The narrow linewidth of the satellite peaks ($n=-1$, full width at half maximum equals 42 in.) indicate that the layer compositions are uniform and the periodicity is highly reproducible. To determine the composition of the well and barrier layers the following procedure was adopted. A thickness ratio of well to barrier of $\frac{1}{4}$ was used as determined from the growth rate. The variation in intensity of the positive and negative satellite peaks turned out to be most sensitive to the strain ratio of the barriers and wells. Only in a small mismatch region a complete suppression of the positive satellites is observed. The lattice mismatch of the $In_{1-x}Ga_xAs$ layers was varied to keep the mean mismatch of the MQW at the measured value of $\Delta a_\perp/a = 1.24\times10^{-3}$. We determined the lattice mismatch of the individual $In_{1-x}Ga_xAs$ and $In_{1-y}Al_yAs$ layer to be $\Delta a_\perp/a = 1.46\times10^{-3}$ and 1.18×10^{-3}, respectively. The small mismatch is accommodated by elastic tetragonal deformation of the layers whose thickness is far below the critical one. The change in interplanar spacing $\Delta a_\perp/a$ perpendicular to the substrate is connected to the chemical composition via the Poisson relation[18] and the related Vegard's law,

$$y_{Al}(x_{Ga}) = \frac{a_{InP}(1+C_{11}/[C_{11}+2C_{12}]\Delta a_\perp/a_{In_{1-y}Al_yAs(In_{1-y}Ga_yAs)}) - a_{InAs}}{a_{AlAs(GaAs)} - a_{InAs}}, \quad (1)$$

where C_{ij} are the elastic stiffnesses of $In_{1-y}Al_yAs$ and $In_{1-x}Ga_xAs$, respectively, and a_{InAs}, a_{AlAs}, a_{GaAs}, and a_{InP} are the room-temperature lattice constants of the binary semiconductor.[19]

The Al and Ga concentrations are found to be $y_{Al}=0.467$ and $x_{Ga}=0.458$. Apparently, the concentration of the $In_{1-y}Al_yAs$ layer is 1.3% and the $In_{1-x}Ga_xAs$ layer 1.0% below for what we expect for lattice-matched conditions.

Now the 2-K low-temperature band-gap energies can be deduced for the $In_{0.533}Al_{0.467}As$ barrier layers from[20]

$$E_g(y) = 1.511 + 2.22(y - 0.48) \text{ eV} \quad (2)$$

to be $E_g = 1.482\pm0.002$ eV, and for the $In_{0.542}Ga_{0.458}As$ layers from[21]

$$E_g(x) = 0.4105 + 0.6337x + 0.475x^2 \text{ eV} \quad (3)$$

to be $E_g = 0.800\pm0.005$ eV.

Crucial information on the subband energy positions is obtained by means of calorimetric absorption spectroscopy (CAS). The CAS signal is the part of the absorbed light power giving rise to phonon emission due to nonradiative recombination processes. Experimental details have been described elsewhere.[22,23] The CAS spectrum is shown in Fig. 2. We clearly observe four transitions at 947, 999, 1132, and 1298 meV. The peaks at 947 and 999 meV are attributed to the excitonic transition of the heavy and light holes $X(e,hh)_{n=1}$ and $X(e,h)_{n=1}$ between the $n=1$ sublevel in the valence band and the $m=1$ sublevel in the conduction band. The steplike behavior at 1298 meV is attributed to excitonic transition between the second $n=m=2$ sublevels $X(e,hh)_{n=2}$. In order to compare these excitonic peak positions with pre-

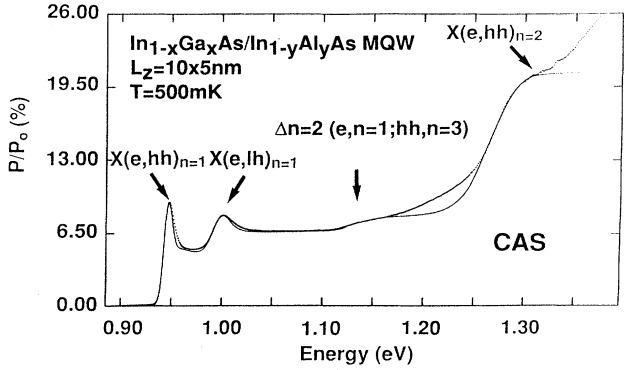

FIG. 2. CAS spectrum of the $In_{1-x}Ga_xAs/In_{1-y}Al_yAs$ $L_z=10\times5$ nm MQW structure; arrows indicate calculated transtion energies. Experimental results are shown as dots and the theoretical line-shape fit as the solid line. $X(e,hh)_{n=1}$, $X(e,lh)_{n=1}$, and $X(e,hh)_{n=2}$ are the excitonic transitions, which fulfill the selection rule $\Delta n=0$, and $\Delta n=2$ $(e,m=1;hh,n=3)$ is the parity-allowed transition.

dictions of band-structure calculations, the following input parameters are used: $E_g(In_{0.533}Al_{0.467}As)=1.482$ eV and $E_g(In_{0.542}Ga_{0.458}As)=0.800$ eV. The nonparabolicity of the conduction bands of $In_{1-x}Ga_xAs$ is described by an energy-dependent effective mass. We use the expression $m_e(E)=m_0(1+2\alpha E)$, where m_0 is the zone-center effective mass and α is 1.135 eV^{-1}, according to Welch, Wicks, and Eastman.[5]

The two-dimensional excitonic transition energy is given by

$$\hbar\omega=E_g+E_C^n(L_z)+E_V^{n,i}(L_z)-E_B^i(L_z) \quad (i=\text{hh,lh},\ n=1,2,\ldots,) \tag{4}$$

where E_g is the 3D band gap of $In_{1-x}Ga_xAs$, E_C^n and $E_V^{n,i}$ are the confinement energies of the electrons and the holes, respectively, and E_B^i is the two-dimensional exciton binding energy. The exciton binding energies are calculated by a variational calculation using an anisotropic wave function and taking into account the effect of image charges. The details are described in Ref. 16.

Furthermore, we consider strain effects on the band structure caused by the lattice mismatch. In our case, the unstrained lattice constant of the $In_{1-x}Ga_xAs$ layers is larger than that of the InP substrate, causing a compressive strain. This strain leads to a symmetry lowering from cubic to tetragonal, which induces a band-gap shift and a change of the valence-band splitting. In the case of biaxial strain parallel to the [010] and [001] directions, the strain-induced band-gap change at the Γ point can be written to first order in the strain[24] neglecting the split-off band as

$$E_{1/2}=E_g+\Delta E\pm 1/2\delta E_{1/2}\ , \tag{5}$$

with a "+" sign for heavy holes and a "−" sign for light holes,

$$\Delta E=2a_H\varepsilon_{xx}(1-C_{12}/C_{11})\ , \tag{6}$$

$$\delta E_{1/2}=-2b_x\varepsilon_{xx}(1+2C_{12}/C_{11})\ , \tag{7}$$

where a_H is the hydrostatic deformation potential, b_s is the shear deformation potential, C_{ij} are the elastic stiffnesses, and ε_{xx} is the strain in (001). The hydrostatic stress component of the strain changes the energy gap by ΔE, while the biaxial component shifts the heavy- and light-hole levels in different directions depending on the sign of the strain. For compressive strain ($\varepsilon_{xx}<0$), Eq. (5) yields a larger heavy-hole–light-hole splitting as compared to unstrained conditions. In our case this change amounts to 4 meV.

The transitions with $n=m$ are very prominent but they are even less dependent on the band discontinuity than the QW eigenenergies. For a variation of the band discontinuity, the energy changes in the conduction- and valence-band sublevels have the opposite signs. In a strained layer system, the selection rule $\Delta n=0$ for optical transition is lifted and only the parity selection rule remains.[25] Mixing of the valence bands is induced.[26] Depending on the amount of strain, the absorption spectrum is still dominated by $n=m$ transitions but new transitions, for example, $\Delta n=2(e,m=1;\text{hh},n=3)$ become allowed. This transition is observed in Fig. 2 at 1132 meV. The energy of this transition is very sensitive to the change of the band discontinuity.

Now we have four experimental transition energies to compare with our band-structure calculations. Only the well width L_z and the conduction-band discontinuity $\Delta E_c/\Delta E_g$ remain as free parameters. The well width determines substantially the absolute energy position while the conduction-band discontinuity influences mainly the valence-band splitting. Therefore, both parameters can be simultaneously and independently determined to be $\Delta E_c/\Delta E_g=(72\pm4)\%$ or $\Delta E_c=504\pm28$ meV and $L_z=4.8\pm0.2$ nm.

The $In_{0.52}Al_{0.48}As$/InP heterostructure exhibits a staggered band lineup. The conduction- and the valence-band edges of $In_{1-y}Al_yAs$ are shifted upward relative to InP. The low-temperature PL spectrum of an $In_{1-y}Al_yAs$/InP heterostructure is shown in Fig. 3. In addition to the near-band-gap emissions from $In_{0.489}Al_{0.511}As$ at 1.581 eV and InP at 1.423 eV a peak at 1.240 eV occurs. This emission is attributed to a spatially indirect transition across the interface due to two-dimensional confined electrons in InP recombining with two-dimensional confined holes in $In_{1-y}Al_yAs$.[27,28] The shoulder at 1.271 eV is attributed to the transition between the $n=m=2$ sublevels of the confined carriers. The potential wells for electrons and holes, respectively, on the two sides of the interface are a consequence of the staggered lineup band structure in the presence of band bending caused by a transfer of electrons from the $In_{1-y}Al_yAs$ layer, with a background doping level of $n=4.8\times10^{17}$ cm^{-3} as determined by capacitance-voltage measurements, to InP. Shubnikov–de Haas (SdH) measurements directly demonstrate the presence of a two-dimensional electron gas at the interface. The sheet electron density is determined to be 6×10^{11} cm^{-2} at $T=4$ K. The inset of Fig. 3 depicts schematically the band structure. To calculate the conduction-band discontinuity from the band-gap energies of the $In_{1-y}Al_yAs$ and InP layers and the indirect interface transition, it is necessary to know the electron and hole confinement energies. These energies are determined by a self-consistent calcu-

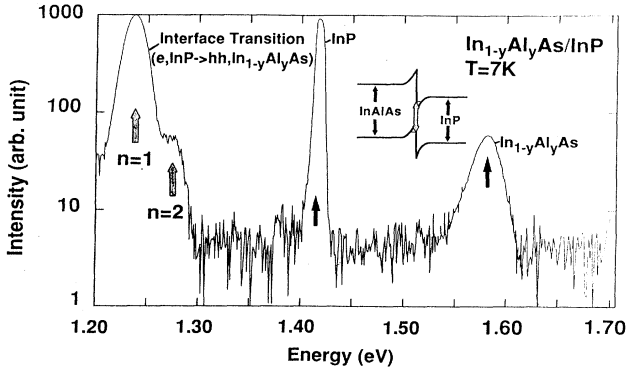

FIG. 3. 7-K PL spectrum of an $In_{1-y}Al_yAs$/InP heterostructure. The inset shows the transitions corresponding to the peaks observed.

lation solving the coupled Schrödinger and Poisson equations at the interface.[29] We determine the $n=1$ electron energy E_e^1 to be 72 meV from the conduction-band minimum and the $n=1$ hole energy E_h^1 to be 40 meV from the valence-band maximum. For the second sublevels we get 102 and 49 meV, respectively. The energy separation between the $n=1$ and 2 sublevels is 39 meV in good agreement with the observed energy separation of 31 meV. From the observed emission energy of the interface transition, the calculated electron and hole eigenenergies, and the band gap of the $In_{1-y}Al_yAs$ layer derived from the emission spectrum, the conduction-band discontinuity of this sample is found to be 453±8 meV or $\Delta E_c=2.86\Delta E_g$ according to Eq. (8),

$$\Delta E_c=E_g(In_{1-y}Al_yAs)-E(\text{interface})+E_e^1+E_h^1 \ . \quad (8)$$

For $In_{0.52}Al_{0.48}As$ perfectly lattice matched to InP the conduction-band discontinuity can be determined to be $\Delta E_c=252\pm8$ MeV using the proportionality $\Delta E_c=2.86\Delta E_g$ and the low-temperature band gap $E_g(I_{0.52}Al_{0.48}As)=1.511$ eV.

One of the most fundamental properties of linear heterojunction models[30–33] is the transitivity. If the conduction-band discontinuity $\Delta E_c(A-B)$ and $\Delta E_c(B-C)$ are known, $\Delta E_c(C-A)$ can be calculated. The resulting equation

$$\Delta E_c(A-B)+\Delta E_c(B-C)-\Delta E_c(C-A)=0 \quad (9)$$

can be used to test our experimental results. Figure 4 shows the flatband energy band diagram for lattice-matched $In_{1-x}Ga_xAs$-$In_{1-y}Al_yAs$-InP-$In_{1-y}Ga_yAs$. Transitivity is satisfied when the band offsets are determined only by the bulk properties of the semiconductors. Failure of transitivity suggests that specific interface effects, such as interface dipole formation, are significantly contributing to the observed band offset. Using our $In_{1-x}Ga_xAs/In_{1-y}Al_yAs$ and $In_{1-y}Al_yAs/InP$ conduction-band discontinuities in conjunction with $\Delta E_c/\Delta E_g=40\pm5\%$ or $\Delta E_c=245\pm20$ meV for $In_{1-x}Ga_xAs/InP$, a value hardly disputed in literature,[34–37] we get

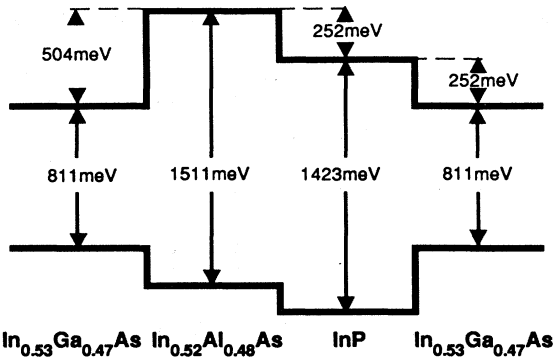

FIG. 4. The low-temperature flatband energy-band diagram of lattice-matched $In_{1-x}Ga_xAs$-$In_{1-y}Al_yAs$-InP-$In_{1-y}Ga_yAs$ with the corresponding conduction-band discontinuities and the band-gap energies.

$$\begin{aligned}\Delta E_c(In_{1-y}Al_yAs/InP)+\Delta E_c(InP/In_{1-x}Ga_xAs)-\Delta E_c(In_{1-x}Ga_xAs/In_{1-y}Al_yAs)&=(252\pm8)\text{ meV}+(245\pm20)\text{ meV}\\&\quad-(504\pm28)\text{ meV}\\&=-7\pm56\text{ meV}\ . \quad (10)\end{aligned}$$

Consequently, within the experimental uncertainty, the band structures at the interfaces of the various samples we have grown are transitive, in agreement with self-consistent tight-binding calculations of Foulon and Priester.[38]

In conclusion, DXD and CAS measurements of $In_{1-x}Ga_xAs/In_{1-y}Al_yAs$ quantum wells are performed to derive the conduction-band discontinuity. Experimental x-ray rocking curves are compared to theoretical ones. This allows a determination of both the lattice mismatch and the corresponding ternary compositions thus providing the necessary input parameters for the interpretation of the optical experiments. The excitonic transition energies including the parity-allowed $\Delta n=2(e,m=1;\text{hh},n=3)$ transition in the CAS spectrum are carefully compared to predictions of band-structure calculations. The conduction-band discontinuity ΔE_c is determined by this analysis to be $\Delta E_c=(0.72\pm0.04)\Delta E_g$. Photoluminescence spectra of $In_{1-y}Al_yAs/InP$ heterostructures show a spatially indirect transition across the interface. The conduction-band discontinuity is derived from a comparison of the energy of this transition with self-consistent band-structure calculations based on results from Shubnikov–de Haas oscillations for lattice-matched $In_{0.52}Al_{0.48}As$ to be $\Delta E_c=252\pm8$ meV. The experimentally determined conduction-band discontinuities fulfill the transitivity rule of the linear heterojunction models.

We would like to thank M. Helm and G. Bauer for the SdH measurements and K. Schatke for expert technical assistance. This work was partially supported by DFG in the framework of SFB6 and by the German Telekom.

[1]H. Temkin, K. Alavi, W. R. Wagner, T. P. Pearsall, and A. Y. Cho, Appl. Phys. Lett. **42**, 845 (1983).

[2]K. Imamura, S. Mato, T. Fujii, N. Yokoyama, S. Hiyamizu, and A. Shibatomi, Electron. Lett. **22**, 1148 (1986).

[3]J. S. Weiner, D. S. Chemla, D. A. B. Miller, T. H. Wood, D. Sico, and A. Y. Cho, Appl. Phys. Lett. **46**, 619 (1985).

[4]K. Shum, P. P. Ho, K. K.Altano, D. F. Welch, G. W. Wicks, and L. F. Eastman, Phys. Rev. B **32**, 3504 (1985).

[5]D. F. Welch, G. W. Wicks, and L. F. Eastman, J. Appl. Phys. **55**, 3176 (1984).
[6]J. Wagner, W. Stolz, and K. Ploog, Phys. Rev. B **12**, 4214 (1985).
[7]J.-H. Huang, T. Y. Chang, and B. Lalevic, App. Phys. Lett. **60**, 733 (1992).
[8]R. People, K. W. Wecht, and K. Alavi, Appl. Phys. Lett. **43**, 118 (1983).
[9]D. V. Morgon, K. Boord, C. E. C. Wood, and L. F. Eastmann, Phys. Status Solidi **72**, 251 (1982).
[10]Y. Sugiyama, T. Inata, T. Fujii, Y. Nakata, S. Muto, and S. Hiyamizu, Jpn. J. Appl. Phys. **25**, 648 (1986).
[11]C. K. Peng, A. Ketterson, H. Morkoc, and P. M. Solomon, J. Appl. Phys. **60**, 1709 (1986).
[12]R. Bhat, M. A. Koza, K. Kash, S. J. Allen, W. P. Hong, S. A. Schwarz, G. K. Chang, and P. Lin, J. Cryst. Growth **108**, 441 (1991).
[13]H. Kroemer and G. Giffiths, IEEE Electron. Device Lett. **EDL-4**, 20 (1983).
[14]L. Aina, M. Mattingly, and L. Stecker, Appl. Phys. Lett. **53**, 1620 (1988).
[15]E. J. Caine, S. Subbanna, H. Kroemer, J. L. Merz, and A. Y. Cho, Appl. Phys. Lett. **45**, 1123 (1984).
[16]D. B. Tran Thoai, R. Zimmermann, M. Grundmann, and D. Bimberg, Phys. Rev. B **42**, 5906 (1990).
[17]A. Segmüller and A. E. Blakeslee, J. Appl. Crystallogr. **6**, 19 (1973).
[18]J. Hornstra and W. J. Bartels, J. Cryst. Growth **44**, 513 (1978).
[19]*Physics of Group IV Elements and III-V Compounds,* edited by O. Madelung, Landolt-Börnstein, New Series, Vol. 17, Pt. a (Springer, Berlin, 1982).
[20]D. Oertel, D. Bimberg, R. K. Bauer, and K. W. Carey, Appl. Phys. Lett. **55**, 140 (1989).
[21]K. M. Goetz and D. Bimberg, J. Appl. Phys. **54**, 4543 (1983).
[22]A. Juhl and D. Bimberg, J. Appl. Phys. **64**, 303 (1988).
[23]D. Bimberg, T. Wolf, and J. Böhrer, in *Advances in Nonradiative Processes in Solids,* Vol. 249 of *NATO Advanced Study Institute, Series B: Physics,* edited by B. DiBartolo (Plenum, New York, 1991), p. 577.
[24]H. Asai and K. Oe, J. Appl. Phys. **54**, 2052 (1983).
[25]R. C. Miller, A. C. Gossard, G. S. Sanders, Yia-Chung Chang, and J. N. Schulman, Phys. Rev. B **32**, 8452 (1985).
[26]G. D. Sanders and Y. C. Chang, Phys. Rev. B **31**, 6892 (1985).
[27]R. Bhat, M. A. Koza, K. Kash, S. J. Allen, W. P. Hong, S. A. Schwarz, G. K. Chang, and P. Lin, J. Cryst. Growth **108**, 141 (1990).
[28]L. Aina, M. Mattingly, and L. Stecker, Appl. Phys. Lett. **53**, 1620 (1988).
[29]S. Haake, R. Zimmermann, D. Bimberg, H. Kal, D. E. Mars, and J. N. Miller, Phys. Rev. B **45**, 1736 (1992).
[30]W. A. Harrison, *Electronic Structure and the Properties of Solids* (Freeman, San Francisco, 1980), p. 252.
[31]R. L. Anderson, Solid State Electron. **5**, 341 (1962).
[32]W. R. Frensley and H. Kroemer, Phys. Rev. B **16**, 2642 (1977).
[33]M. Tersoff, Phys. Rev. B **30**, 4874 (1984).
[34]D. V. Lang, M. B. Panish, F. Capasso, J. Allam, R. Hamm, A. M. Sergent, and W. T. Tsang, Appl. Phys. Lett. **50**, 736 (1987).
[35]M. Razeghi, J. P. Hirtz, U. O. Ziemelis, C. Delalonde, B. Etienne, and M. Voos, Appl. Phys. Lett. **43**, 585 (1983).
[36]S. R. Forrest, P. H. Schmidt, R. B. Wilson, and M. L. Kaplan, Appl. Phys. Lett. **45**, 1199 (1984).
[37]S. R. Forrest and O. K. Kim, J. Appl. Phys. **53**, 5738 (1982).
[38]Y. Foulon and C. Priester, Phys. Rev. B **45**, 6259 (1992).